Numerical Predictions of Rotor Performance using a Navier-Stokes Simulation coupled with a Time-Marching Free-Wake Model

Kihoon Chung*, Kwanjung Yee and Changjeon Hwang****
Rotorcraft Department, Rotorcraft Development Division,
Korea Aerospace Research Institute, Daejeon, Korea, 305-311

Duckjoo Lee***
Division of Aerospace Engineering,
Korea Advanced Institute of Science of Technology, Daejeon, Korea, 305-701

Abstract

CFD method has been coupled with a time-marching free-wake model by using field velocity approach suggested by J. D. Baeder (Ref. 1). The coupled method has been applied to rectangular and BERP-like blades and the calculated performance data are compared with the experimental results.

For hovering analysis, the present method could yield sufficiently good results with reasonable computation time and is particularly suitable for the flow field analysis with the complex shaped blade.

Key Word : Rotor performance prediction, Navier-Stokes, Time-marching free-wake, Field velocity approach

Introduction

The accurate prediction of aerodynamic loads and performance of a hovering rotor continues to be one of the most complex and challenging problems. The dominant key of these complex and challenging problems is vortical wake, which strongly influences the operating characteristics of helicopters. The accurate prediction of this vortical wake is the most important, the most studied, and the most difficult aspect of the flow-field.

The current methods of predicting hovering rotor flow field range in complexity from relatively simple blade element method to more sophisticated computational fluid dynamics(CFD, hereafter) methods. Although it is hoped that CFD methods eventually will replace all the simple methods for performance evaluation, there is still a long way to go due to the following constraints. One is the numerical diffusion which prevents the accurate prediction of formation and convection of the vertical wake. The other is extremely large computer resources and computation time required for CFD simulation of rotor wake based on first principles. Various semi-empirical methods are currently being used in the helicopter industry to predict airloads. Empirical methods intrinsically require external wake models for realistic estimates of airloads, which limit their application to the blades with more complex geometry such as BERP. One of the most critical limitations of empirical methods is that they are not capable of simulating the

* Post-Doctorial Fellow
E-mail : khchung@kari.re.kr, Tel : 042-860-2283, Fax : 042-860-2604
** Senior Researcher
*** Professor

detailed physics of near- field aerodynamics around rotor blade with unconventional geometry.

CFD methods coupled with a wake model could be a good alternative to the previous constraints of CFD and semi-empirical methods (Ref. 1). In this paper, CFD method has been coupled with a time-marching free-wake model by using field velocity approach. The primary objective of the present research is to assess the accuracy of the present method when applied to the analysis of flow-field around rotor blade with complex geometry like BERP (Ref. 2).

Numerical Method

Time-marching Free-wake Method

The fluid surrounding the body is assumed to be inviscid, irrotational, and incompressible over the entire flow field, excluding the body's solid boundaries and its wakes. Therefore, a velocity potential $\Phi(\vec{x}, t)$ can be defined and the continuity equation in the inertial frame becomes:

$$\nabla^2\Phi = 0 \tag{1}$$

The boundary condition requiring zero normal velocity across the body's solid boundaries is:

$$(\nabla\Phi + \vec{V}_{wake} - \vec{V}) \cdot \vec{n} = 0 \tag{2}$$

Where $\vec{V}_{wake}(\vec{x}, t)$ is the induced velocity due to the vorticity field in the wake, $\vec{V}(\vec{x}, t)$ is the body surface's velocity, and $\vec{n}(\vec{x}, t)$ is the vector normal to the moving surface, as viewed from the blade.

Using Green's second identity, the general solution of equation (1) can be constructed by integrating the contribution of the basic solution of source (σ) and doublet (μ) distributions over the body's surface:

$$\Phi(\vec{x}, t) = \frac{1}{4\pi}\int_{body+wake} \mu\,\vec{n}\cdot\nabla\left(\frac{1}{r}\right)ds - \frac{1}{4\pi}\int_{body}\sigma\left(\frac{1}{r}\right)ds \tag{3}$$

Inserting equation (3) into equation (2) becomes:

$$\left\{\frac{1}{4\pi}\int_{body+wake}\mu\nabla\left[\frac{\partial}{\partial n}\left(\frac{1}{r}\right)\right]ds - \frac{1}{4\pi}\int_{body}\sigma\left(\frac{1}{r}\right)ds - \vec{V}\right\}\cdot\vec{n} = 0 \tag{4}$$

The source term is neglected in the case of the thin blade. Thus, only the first part of equation (3) is used to represent the lifting surface. The constant-strength doublet panel is equivalent to a closed vortex lattice with the same strength of circulation, ($\Gamma = \mu$). Then the induced velocity of the vortex lattice in equation (4), representing the blade, can be obtained by using Biot-Savart's law:

$$\vec{V} = -\frac{1}{4\pi}\int_{c}\frac{\vec{r}\times\Gamma d\vec{l}}{|\vec{r}|^3} \tag{5}$$

The collocation point is located at the mid-span and three-quarter chord of each panel. The boundary condition of no-flow penetration is satisfied at the collocation point of each lattice. The application of the flow tangency condition (equation 4) to the vortex lattice distribution yields the following linear matrix equation that is to be solved:

$$A_{ij}\Gamma_j = R_i \qquad (i, j = 1, n) \tag{6}$$

where A_{ij} is the coefficient matrix of normal induced velocity on the i-th element of the blade due to the j-th vortex lattice with the unit circulation, and Γ_j is the unknown circulation

value of the blade vortex lattice. R_i is the normal induced velocity at each control point due to the free stream velocity, the blade-moving velocity, and the wake-induced velocity.

A three-dimensional wing trails the bound circulation(Γ) into the wake. Radial variation of bound circulation produces trailed vorticity in the wake, which is parallel to the local free stream direction at each instant when it leaves the blade. Azimuthal variation of bound circulation produces shed vorticity, oriented radially in the wake. The strengths of the trailed and shed vorticity are determined by the radial and azimuthal derivatives of bound circulation at the time the wake element leaves the blade. The bound circulation has a peak near the tip, and quickly drops to zero. The trailed sheet therefore has a high strength(proportional to the radial derivative of Γ) at the outer wake, and quickly rolls up into a concentrated tip vortex. The strength of the trailed shed wake vortex at this time step is set equal to the one of the vortex lattice elements, which is located at the trailing edge of the blade($\Gamma_{T.E.,t} = \Gamma_{wake,t}$). This condition is forced to satisfy the Kutta condition($\gamma_{T.E.} = 0$).

Since the wake surface is force-free, each vortex wake element moves with the local stream velocity, which is induced by the other wake element and the blade. The convection velocity of the wake is calculated in the inertial frame. The vortex wakes are generated at each time step. Therefore, the number of wake-elements increases as the blade is rotating. It is clear that a large number of line elements for the highly curved and distorted wake region like the tip vortex are required to describe the vortex filament distortions accurately. In general, computational time for the calculation of the wake distortion is proportional to the square of the vortex element number. Therefore, a parabolic blending curved element is used to describe the highly curved and distorted vortex and to reduce the number of elements (Refs. 4 & 5).

Navier-Stokes Analysis

The governing differential equations are the thin layer Navier-Stokes equations. These can be written in conservation law form in a generalized coordinate system as follows:

$$\partial_\tau \hat{Q} + \partial_\xi \hat{E} + \partial_\eta \hat{F} + \partial_\zeta \hat{G} = \frac{1}{Re}\partial_\zeta \hat{S} + \hat{R} \tag{7}$$

The coordinate system (x, y, z, t) is attached to the blade. The vector of conserved quantities $\hat{Q}$ and the inviscid flux vectors $\hat{E}$, $\hat{F}$ and $\hat{G}$ are given by

$$\hat{Q} = \frac{1}{J}\begin{bmatrix} \rho \\ \rho u \\ \rho v \\ \rho w \\ e \end{bmatrix}, \hat{E} = \frac{1}{J}\begin{bmatrix} \rho U \\ \rho uU + \xi_x p \\ \rho vU + \xi_y p \\ \rho wU + \xi_z p \\ UH - \xi_t p \end{bmatrix}, \hat{F} = \frac{1}{J}\begin{bmatrix} \rho V \\ \rho uV + \eta_x p \\ \rho vV + \eta_y p \\ \rho wV + \eta_z p \\ VH - \eta_t p \end{bmatrix}, \hat{G} = \begin{bmatrix} \rho W \\ \rho uW + \zeta_x p \\ \rho vW + \zeta_y p \\ \rho wW + \zeta_z p \\ WH - \zeta_t p \end{bmatrix} \tag{8}$$

In these equation, $H = (e+p)$, U, V and W are the contravariant velocity component defined, for example, as $U = \xi_t + \xi_x u + \xi_y v + \xi_z w$. The cartesian velocity components are given by u, v, and w in the x, y, and z directions, respectively. Also, the density, pressure, and total energy per unit volume are represented by ρ, p, and e, respectively. Whereas the velocity and length scales are non-dimensionalized by the characteristic velocity and length scales, given by the ambient sound speed a_∞ and the rotor blade chord c, the pressure p, density ρ, and the energy e are non-dimensionalized by the free-stream reference values p_∞/γ, ρ_∞, and $\rho_\infty a_\infty^2$, respectively. The quantities ξ_x, ξ_y, ξ_z, ξ_t, etc., are the coordinate transformation metrics, and J is the Jacobian of the transformation. For the thin-layer approximation used here, the viscous flux vector $\hat{S}$ is given by

$$\hat{S}=\frac{1}{J}\begin{bmatrix}0\\ \mu m_1 u_\zeta+\mu/3\, m_2\zeta_x\\ \mu m_1 v_\zeta+\mu/3\, m_2\zeta_y\\ \mu m_1 w_\zeta+\mu/3 m_2\zeta_z\\ \mu m_1 m_3+\mu/3 m_2(\zeta_x u+\zeta_y u+\zeta_z w)\end{bmatrix} \tag{9}$$

With

$$m_1=\zeta_x^2+\zeta_y^2+\zeta_z^2$$

$$m_2=\zeta_x u_\zeta+\zeta_y v_\zeta+\zeta_z w_\zeta$$

$$m_3=\frac{1}{2}(u^2+v^2+w^2)_\zeta+\frac{1}{Pr(\gamma-1)}(a^2)_\zeta$$

where Pr is the Prandtle number, γ is the ratio of specific heats, and a is the speed of sound.

The fluid pressure p is related to the conserved flow quantities through the non-dimensional equation of state for a perfect gas given by

$$p=(\gamma-1)\left\{e-\frac{\rho}{2}(u^2+v^2+w^2)\right\} \tag{10}$$

For turbulent viscous flows the non-dimensional viscosity coefficient μ in $\hat{S}$ is computed as the sum of $\mu_l+\mu_t$, where the laminar viscosity, μ_l, is estimated using Sutherland's law and the turbulent viscosity, μ_t, is evaluated using the Baldwin-Lomax algebraic eddy viscosity model.

Roe's finite difference method is employed for the spatial discretization of the convective flux terms. MUSCL interpolation with a flux limiter is used to obtain higher order spatial accuracy. For temporal integration, LU-SGS method has been employed. All boundary conditions are applied explicitly for computational efficiency.

Field Velocity Approach

N-S analysis has been coupled with a time-marching free-wake model as shown in Fig. 1 by using field velocity approach suggested by J. D. Baeder (Ref. 1). The field velocity approach lies between the perturbation and surface transpiration method in terms of computation time and complexity of algorithm. The induced velocity due to vortical wake is included via time metric terms.

$$x_\tau\vec{i}+y_\tau\vec{j}+z_\tau\vec{k}=\vec{\Omega}\times\vec{r}-\vec{V_w} \tag{11}$$

where $\vec{V_w}$ is the wake-induced velocity. Although this approach neglects the effect of vortex pressure and density fields, it requires less memory than the perturbation method and is easily applied to viscous flow simulation unlike surface transpiration approach.

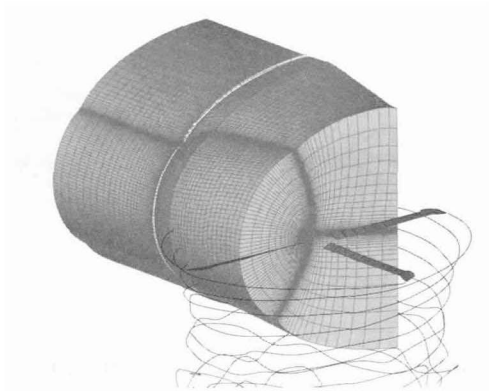

Fig. 1. Schematics of the coupled analysis

For convenience, the coupling method is classified in terms of the way of data feedback between free-wake analysis and CFD analysis. In the loosely coupled method(LCM, hereafter), the induced velocity obtained from free-wake analysis is fed into CFD code only once. In other words, there is no iteration or feedback between CFD analysis and free-wake analysis. On the other hand, the induced velocity is iteratively updated in tightly coupled method(TCM, hereafter). The two algorithms are compared in Fig. 2.

In this paper, the loosely coupled method is used to predict the performance of hovering rotor.

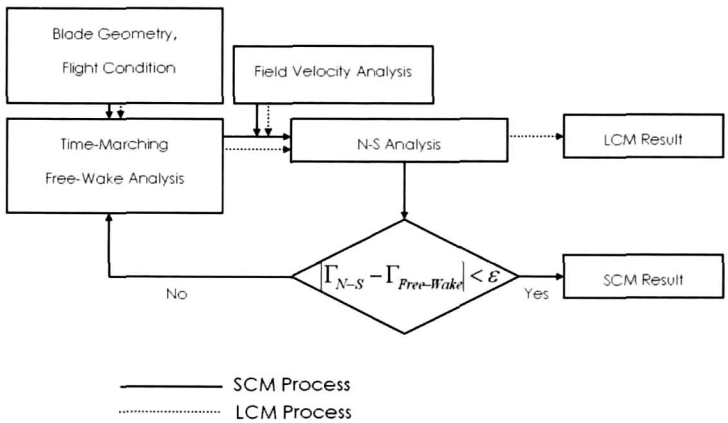

Fig. 2. Flow chart of coupled methods

RESULTS

Predictions of Tip Vortex Trajectories

In order to show the capability of wake capturing, two cases of the wake geometry are calculated using a time-marching free-wake analysis. One of the wake computations is the same as that investigated in the experiments of Caradonna and Tung (Ref. 5). Twenty-four time-steps were taken per blade revolution and the vortex core radius is taken as 10% of the chord length that is commonly used in rotor wake simulations (Ref. 6).

Fig. 3 shows the calculated rotor and trailed wake geometries. Fig. 4 shows the calculated values of the radial and axial locations of tip vortex are compared with the experiment results (Ref. 5). The calculated tip-vortex geometries show good agreement with the experiment results.

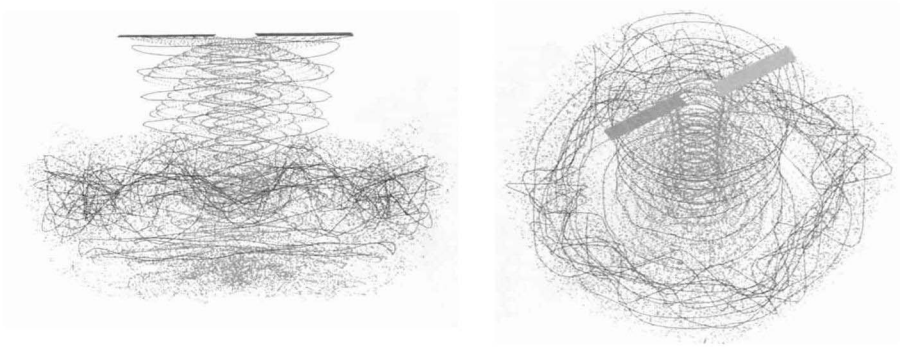

(a) Side View (b) Quater View

Fig. 3. Blade and wake geometries calculated by using a time-marching free-wake method

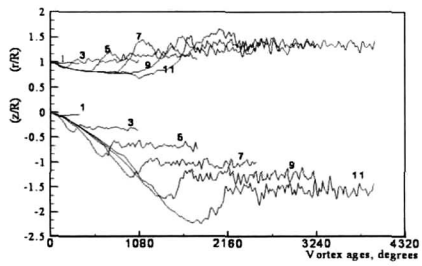

(a) Time history of tip-vortex position

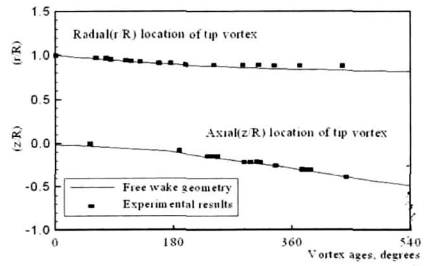

(b) Tip-vortex geometry at 10 revolutions

Fig. 4. Comparison of the tip vortex axial and radial locations between the free wake and experimental results (Experimental data from Ref. 5)

Secondly, the wake geometry of the rotor investigated in the experiments of Caradonna et al and Komerath et al (Ref. 7) is calculated. The trajectories of the tip vortices for collective angle of 11^o at a climb rate of 3.5 ft/s are shown in Fig. 5. The tip vortex trajectories from the two blades are offset by 180^o and it is clear that they are influencing each other. The first interaction of the z/R(axial direction) curves of the two vortices indicates the beginning of the vortex pairing process. Subsequent crossings indicate the rotation of the two vortices about each other. In this case, the results of the time-marching free-wake method show good agreement with the radial(r) and downstream(z) distance positions, and shows that the tip-vortex pairing occurs at $\zeta = 720^o$, which is the same as the experimental data (Ref. 7).

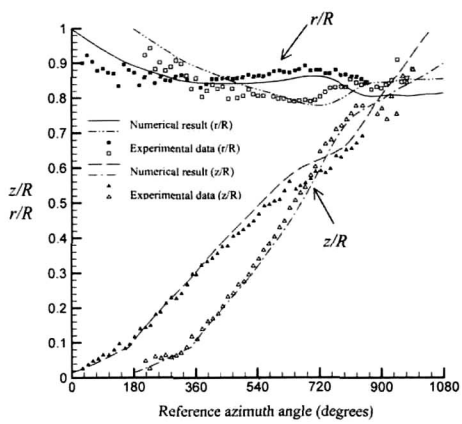

Fig. 5. Wake geometries at 11^o collective angle, 3.5 ft/s climb rate (Experimental data from Ref. 7)

Predictions of Performance

In this paper, the loosely coupled method has been applied to rectangular and BERP-like blade and the calculated performance data are compared with the experimental results.

Fig. 6 shows the blade surface grids of rectangular and BERP-like rotor. Body-conforming, single block, three dimensional computational grids were constructed for the both rotors by stacking C-H grids as shown in Fig. 7. The computational field grid used has 121 grid points in the wraparound (along the chord) direction, 71 points in the spanwise(radial) direction, and 41

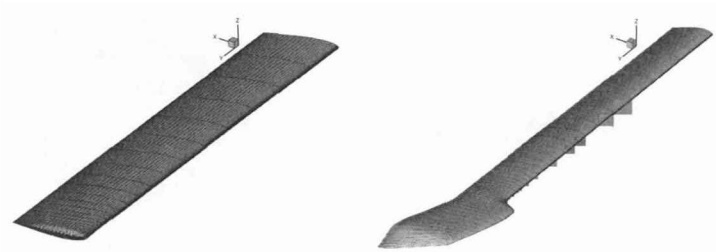

(a) Rectangular blade (b) Berp-like blade

Fig. 6. Surface grids of blades

points in the normal direction.

First, in order to validate the overall accuracy of the present coupled approach, calculations were performed for rectangular blade and the results are compared with the experimental data of Caradonna and Tung (Ref. 5). Fig. 8 shows the Cp distributions at various spanwise positions. The computation results of N-S simulation coupled with a time-marching free-wake show good agreements with experiment at various spanwise locations. It should be noted that the shock location and 3-D effect at the tip regions are captured with good accuracy. The dashed lines of Fig. 8 are the results of J. D. Baeder (Ref. 1). The wake models of J. D. Baeder's calculation are Kocurek's prescribed wake model (Ref. 9) and known tip-vortex strength as given by Beddoe's model (Ref. 10). But the wake models, used by J. D. Baeder, over-predicted the radial contraction comparing with Caradona and Tung's experiments (See Ref. 1). It appears that by coupling CFD method with a time-marching free-wake, more accurate cp distributions and performance of the blade can be predicted mainly due to the fact that time marching free-wake model can accurately predict the tip-vortex trajectory and strength.

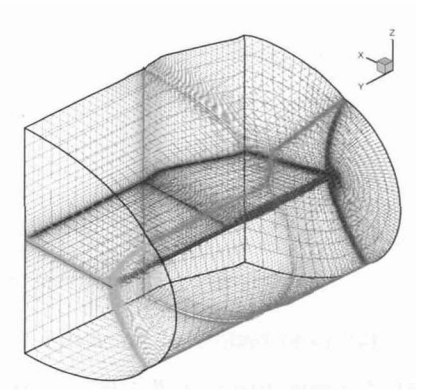

Fig. 7. Field grid of BERP-like blade

The present method has been applied to the calculation of hovering performance of

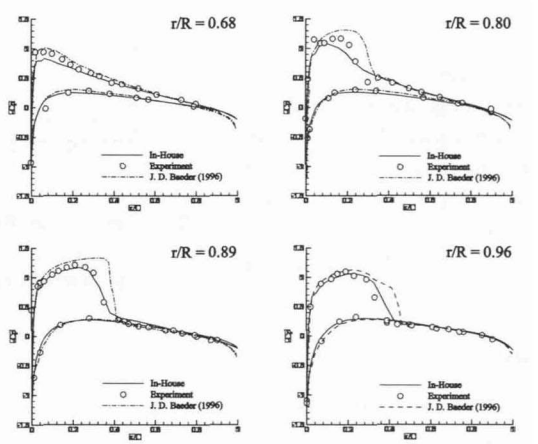

Fig. 8. Comparison of C_p for $\theta_c = 8^o$, $M_{tip} = 0.877$ and $Re_c = 3.93 \times 10^6$

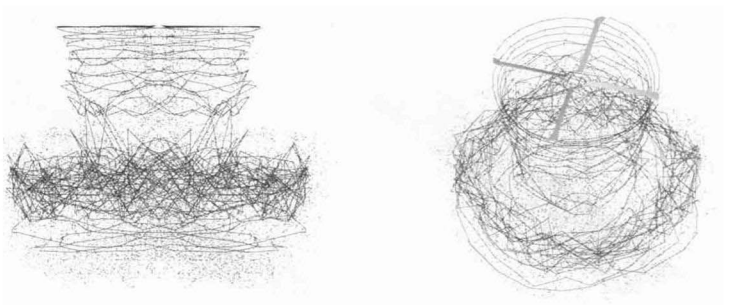

(a) Side view (b) Quarter view

Fig. 9. Wake geometry of time-marching free-wake for $\theta_c = 8^o$, $M_{tip} = 0.643$

BERP-like blade. The detailed blade geometry can be found in Ref. 2. Fig. 9 shows the rotor and wake geometries of a BERP-like rotor calculated by using a time-marching free-wake method.

Fig. 10 shows comparison of predicted and measured C_T vs. C_Q of Ref. 2. As can be found in the figure, predicted results are in good agreement with experiment. The predicted FM verses $C_T^{1.5}/\sigma$ are shown in Fig. 11. The predicted performance results show good agreement with experimental data.

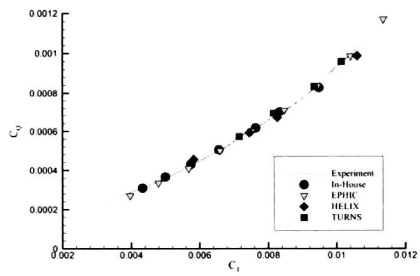

Fig. 10. Comparison of measured and predicted C_T versus C_Q results (Experiment, EPHIC, HELIX, TURNS data from Ref. 2)

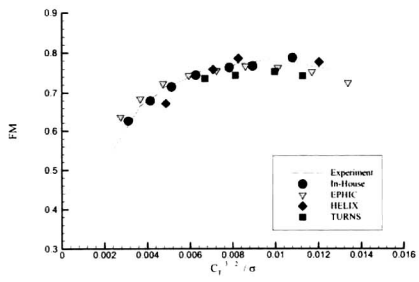

Fig. 11. Comparison of measured FM with predicted FM (Experiment, EPHIC, HELIX, TURNS data from Ref. 2)

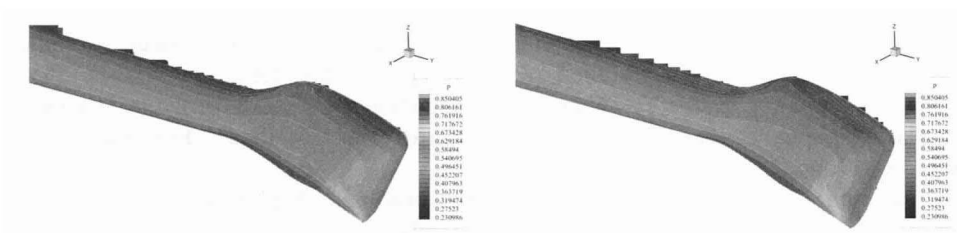

(a) 5^o Collective angle at 0.75R (b) 9^o Collective angle at 0.75R

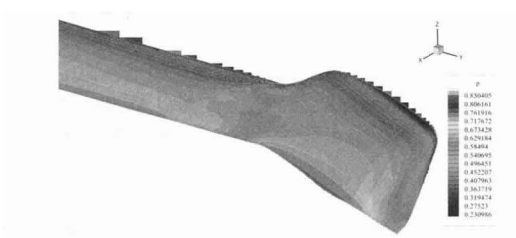

(c) 11^o Collective angle at 0.75R

Fig. 12. Pressure contours of upper surface at various collective angle, $M_{tip} = 0.643$

Fig. 12 shows the pressure contour of upper surface of BERP-like rotor at various collective angles. At high collective angle, the pressure contour around the notch of a BERP-like rotor shows an additional vortex generated at the notch of BERP-like rotor as shown in Fig. 12(c). This numerical method is fairly efficient in terms of computational cost and runs at Pentium 4 PC with 512 MB memory. The total computation for each case including time-marching free-wake and N-S analysis takes about 3 hours of CPU time

Conclusions

In this paper, CFD method has been coupled with a time-marching free-wake model by

using field velocity approach. The coupled method has been applied to rectangular and BERP-like blade and the calculated performance data are compared with the experimental results.

The conclusions by now are: 1) for hovering analysis LCM could yield sufficiently good results with reasonable computation time; 2) the present method is particularly suitable for the flow field analysis with complex shaped blade.

In future, the researches about forward flight and BVI by using a strongly coupled method will be performed.

Acknowledgement

This research was sponsored by "Innovative Technology Study for the Jet-Smooth Quiet Rotor System" project which is one of "National Research Laboratory Programs" supported by Ministry of Science and Technology of the Republic of Korea.

References

1. Harsh Khanna and James D. Baeder, "Coupled Free-Wake/CFD Solutions for Rotors in Hover Using a Field Velocity Approach", 52nd Annual Forum of AHS, Washington D. C., June 4-6, 1996.

2. Chee Tung and Soogab Lee, "Evaluation of Hovering Performance Prediction Codes", 50thAnnual Forum of AHS, Washington D.C., May 11-13, 1994.

3. Ryu, K. W. and Lee, D. J., "Sound radiation from elliptic vortex rings: evolution and interaction", Journal of sound and vibration, Vol. 200, pp. 281-301, 1997.

4. Na, S. U. and Lee, D. J., "Numerical Simulations of Wake Structure Generated by Rotating Blades Using a Time-Marching Free-Vortex-Blob Method", European Journal of Mechanics, 18, (1), pp. 147~159, 1999.

5. Caradonna, F. X. and Tung, C., "Experimental and Analytical Studies of a Model Helicopter Rotor in Hover", NASA TM 81232 , September, 1981.

6. Leishman, J. G., Baker, A., Coyne, A., "Measurements of Rotor Tip vortices Using Three-Component Laser Doppler Velocimetry", J. American Helicopter Society, 41, (4), Oct., pp. 342~353, 1996.

7. Caradonna, F., Hendley, E., Silva, M., Huang, S., Komerath, N., Reddy, U., Mahalingam, R., Funk, R., Ames R., Darden, L., Villareal, L., Gregory, and Wong, O., "An Experimental Studyof a Rotor In Axial Flight", AHS Specialists' Meeting on Aerodynamics and Aeroacoustics, Williamsburg, VA, Oct., 1997.

8. Chung, K. H., Na, S. U., Jeon, W. H., Lee, J., "A Study on Rotor Tip-Vortex Pairing Phenomena by using Time-Marching Free-Wake Method", American Helicopter Society 56th Annual Forum, Virginia Beach, Virginia, May 2-4, D. 2000.

9. Kocurek, J. D. and Tangler, J. L., "A Prescribed Wake Lifting Surface Hover Performance Analysis", American Helicopter Society 32nd Annual Forum, May, 1976.

10. Beddoes, T. S., "A Wake Model For High Resolution Airloads", the 2nd International Conference on Basic Rotorcraft Research, Triangle Park, NC, 1985.